International Journal of Advanced Research in Physical Science (IJARPS)
Volume 2, Issue 8, August 2015, PP 35-46
ISSN 2349-7874 (Print) & ISSN 2349-7882 (Online)
www.arcjournals.org

Three-Dimensional Free Convection Around an Inclined Cone of Revolution

Ulrich CANISSIUS*

Laboratoire de Mécanique et de Métrologie,
Ecole Normale Supérieure pour l'Enseignement Technique (ENSET), Université d'Antsiranana
B.P.0, Antsiranana 201, Madagascar
canissiusulrich@yahoo.fr

Edouard ALIDINA

Laboratoire de Mécanique des Fluides et Systèmes Energétiques Appliqués (LMFSEA)
Faculté des Sciences, Université d'Antsiranana
B.P.0, Antsiranana 201, Madagascar

Abstract: *This work is devoted to a numerical study of the thermal free convection, laminar and permanently developed in the vicinity of a smooth-walled truncated cone. The equations governing these transfers are developed in the framework of the approximation of the laminar boundary layer.*

Authors numerically solving, using the method of finite differences, the transfer equations, laminar, three-dimensonal, between inclined isothermal cone of revolution, and a newtonian fluid in vertical upward flow generated by the free convection. In the boundary layer, the results concerning the adimensional velocity fields and temperatures as well as the Nusselt numbers and the friction coefficients, are represented graphically.

Keywords: *three-dimensional free convection, three-dimensional boundary layer, inclined cone of revolution, momentum and heat transfers, theorical study.*

1. NOMENCLATURE

1.1. Roman Letter Symbols

a thermal diffusivity of the fluid, $(m^2.s^{-1})$

Cf_u meridian friction coefficient

Cf_w azimuthal friction coefficient

Cp specific heat capacity at constant pressure of the fluid, $(J.kg^{-1}.K^{-1})$

g acceleration due to gravity $(m.s^{-2})$

L reference length equal to the length of the generatrix of the cone, (m)

Nu local Nusselt number

Pr Prandtl number

r normal distance from the projected M of a point P of the fluid to the axis of revolution of cone,(m)

S_x, S_φ factors of geometric configuration

T_∞ temperature of the fluid away from the wall, (K)

T_p temperature of the wall, (K)

V_x velocity component in x-direction, $(m.s^{-1})$

V_y velocity component in y-direction, $(m.s^{-1})$

V_φ velocity component in φ-direction, $(m.s^{-1})$

x meridian coordinate, (m)

y normal coordinate, (m)

1.2. Greek Letter Symbols

α angle of inclination, (°)

φ azimuthal coordinate, (°)

ρ density of the fluid, $(kg.m^{-3})$

θ_o half angle of the cone, (°)

ν kinematic viscosity, ($m^2.s^{-1}$)

λ thermal conductivity, ($W.m^{-1}.K^{-1}$)

μ dynamic viscosity, ($kg.m^{-1}.s^{-1}$)

β Volumetric coefficient of thermal expansion, (K^{-1})

1.3. Indices/ Exponents

$+$ dimensionless variables

2. Introduction

Various applications of heat transfer in the vicinity of the body symmetrical raised many theoretical and experimental studies both because of their importance in many areas of technology (thermal power plants, solar collectors, heat exchangers, ...).

Much work has been published on the free convection around a vertical cone as well as its wall is uniform or not, it is maintained at a constant temperature or subjected to a heat flux.

Merk and Prins [1] developed the general relationship on the solutions of an axisymmetrical system of an isothermal body and discussed a study of the laminar thermal convection type boundary layer in the vicinity of a cone with a smooth surface. Alamgir [2] investigated the overall heat transfer in laminar free convection from vertical cones using the integral method. Bapuji et al. [3] studied the current unstable of the laminar natural convection with an isothermal vertical cone. Pop and Tsung Yen [4] have studied the effects of the compressibility in the laminar convection around a vertical cone and shown that the heat transfer for a smooth-walled cone are superior to those obtained for a corrugated wall cone, and again later Siabdallah et al. [5] confirmed this phenomenon. S. Roy [6] studied this transfer by free convection around a vertical cone but with a very high Prandtl number. Having regard to all these works on a vertical cone, the study of heat transfer about an inclined cone, is also of great interest. Recently, F.A. Rakotomanga et al. [8] have approached the study of the influence of the angle inclination of the cone on the flow and heat transfer between the wall and the fluid by forced convection. They have shown that, on one hand, increasing the angle inclination reduces the heat exchange between the fluid and the wall, but on other hand it causes a slight increase in the thickness of the boundary layer. This work, which aims to analyze the effect on the heat transfer of the cone angle inclination and its opening angle, the latter provides a numerical study of natural convection.

The conservation equations are discretized using an implicit finite difference scheme. The Velocity fields and temperatures, associated with the boundary conditions, are determined from the Thomas algorithm.

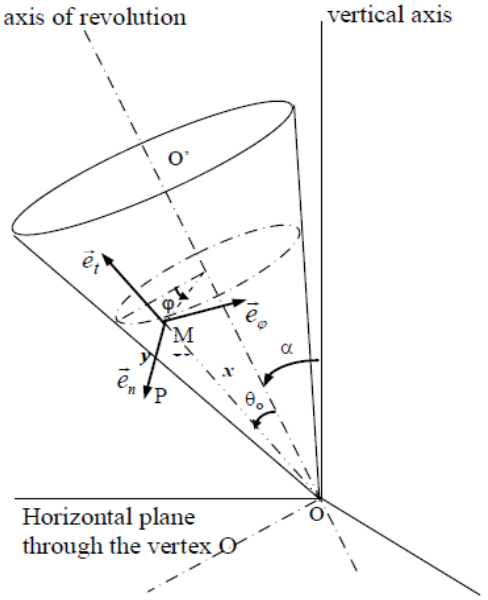

Fig1. *Physical model and co-ordinates system*

3. MATHEMATICAL FORMULATION

The physical model considered consists of a cone of revolution of length L and inclined at an angle α relative vertically. The wall of the cone is kept at a temperature constant Tp, different of the temperature T∞ of fluid away from the wall which is also constant.

3.1. Simplifying Assumptions

Besides the classical assumptions of the boundary layer and those of Boussinesq,we ask the following assumptions:

- The cone is stationary,
- Transfers are laminar and permanent
- Radiative transfer and viscous dissipation of energy are negligible,
- The fluid is air whose physical properties are constant except for the density of which is to change the origin of the natural convection.

3.2. Conservation Equations in the Boundary Layer

Using the following dimensionless variables:

$$x_+ = \frac{x}{L},\ y_+ = \frac{y}{L}Gr^{\frac{1}{4}},\ \varphi_+ = \varphi,\ r^+ = \frac{r}{L},\ V_x^+ = \frac{V_x}{\sqrt{Lg\beta\Delta T}},$$

$$V_y^+ = \frac{V_y Gr^{\frac{1}{4}}}{\sqrt{Lg\beta\Delta T}},\ V_\varphi^+ = \frac{V_\varphi}{\sqrt{Lg\beta\Delta T}},\ T^+ = \frac{T - T_\infty}{T_P - T_\infty}$$

with $Gr = \frac{g\beta(T_p - T_\infty)L^3}{\nu^2}$, Grashof number

The governing boundary layer equations of continuity, momentum and energy under Boussinesq approximation are as follows:

3.3. Equation of Continuity

$$\frac{\partial V_x^+}{\partial x_+} + \frac{\partial V_y^+}{\partial y_+} + \frac{1}{r^+}\frac{\partial V_\varphi^+}{\partial \varphi_+} + \frac{V_x^+}{r^+}\frac{dr^+}{dx_+} = 0 \tag{1}$$

3.4. Equation of Momentum

$$V_x^+\frac{\partial V_x^+}{\partial x_+} + V_y^+\frac{\partial V_y^+}{\partial y_+} + \frac{V_\varphi^+}{r^+}\frac{\partial V_x^+}{\partial \varphi_+} - \frac{V_\varphi^{+2}}{r^+}\frac{dr^+}{dx_+} = S_x T^+ + \frac{\partial^2 V_x^+}{\partial y_+^2} \tag{2}$$

$$V_x^+\frac{\partial V_\varphi^+}{\partial x_+} + V_y^+\frac{\partial V_\varphi^+}{\partial y_+} + \frac{V_\varphi^+}{r^+}\frac{\partial V_\varphi^+}{\partial \varphi_+} + \frac{V_x^+ V_\varphi^+}{r^+}\frac{dr^+}{dx_+} = S_\varphi T^+ + \frac{\partial^2 V_\varphi^+}{\partial y_+^2} \tag{3}$$

S_x and S_φ designate the factors of geometric configuration defined by:

$$S_x = \sin\alpha.\cos\varphi.\sin\theta_0 + \cos\alpha.\cos\theta_0 \tag{4}$$

$$S_\varphi = -\sin\alpha.\sin\varphi \tag{5}$$

3.5. Equation of Energy

$$V_x^+\frac{\partial T^+}{\partial x_+} + V_y^+\frac{\partial T^+}{\partial y_+} + \frac{V_\varphi^+}{r^+}\frac{\partial T^+}{\partial \varphi_+} = \frac{1}{Pr}\frac{\partial^2 T^+}{\partial y_+^2} \tag{6}$$

with $Pr = \frac{\mu \ Cp}{\lambda} = \frac{\nu}{a}$, Prandtl number

In these equations, we associate the following dimensionless boundary conditions:

on the wall, $y^{+} \to 0$

$$T^{+} = 1, \ V_{x}^{+} = V_{y}^{+} = V_{\varphi}^{+} = 0 \tag{7}$$

away of the wall, $y^{+} \to \propto$:

$$T^{+} = 0, \ V_{x}^{+} = V_{y}^{+} = V_{\varphi}^{+} = 0 \tag{8}$$

2.3. Nusselt number and friction coefficients

2.3.1. Nusselt Number

$$NuGr^{-\frac{1}{4}} = -\left(\frac{\partial T^{+}}{\partial y_{+}}\right)_{y_{+}=0} \tag{9}$$

2.3.2. Friction Coefficients

$$\frac{1}{2} Cf_{u} Gr^{\frac{1}{4}} = \left(\frac{\partial V_{x}^{+}}{\partial y_{+}}\right)_{y+=0} \tag{10}$$

$$\frac{1}{2} Cf_{w} Gr^{\frac{1}{4}} = \left(\frac{\partial V_{\varphi}^{+}}{\partial y_{+}}\right)_{y+=0} \tag{11}$$

4. NUMERICAL SOLUTION

The study area is divided into N x M x L curvilinear parallelepiped attached to the body and defined by the steps dimensionless Δx_{+}, Δy_{+} and $\Delta\varphi_{+}$, N and L being the number of meridians and parallels. For clarity, we note respectively U, V, W and T the meridional, normal, azimuthal and dimensionless temperature. the dimensionless conservation equations (1), (2), (3) and (6) are discretized using an implicit finite difference scheme. The calculations are performed at the nodes (i,j,k) with $1 \le i \le N$, $1 \le j \le M$ and $1 \le k \le L$. After arrangement, the discretized equations can each be written in the following form: $A X_{j+1} + B X_{j} + C X_{j-1} = D_{j}$, $\quad 2 \le j \le JMAX - 1$ (12)

wherein X is chosen from one of the variables U, W and T, JMAX index characterizing the thickness of the boundary layer. The algebraic systems (12) associated with the discretized boundary conditions are solved by the Thomas algorithm. As for the dimensionless normal component is calculated from the continuity equation:

$$V_{i+1,j}^{k} = \frac{1}{4}\left[3V_{i+1,j+1}^{k} + V_{i+1,j-1}^{k} + 2\Delta y_{+}\left(\frac{U_{i+1,j}^{k} - U_{i,j}^{k}}{\Delta x_{+}} + \frac{3W_{i+1,j}^{k+1} - 4W_{i+1,j}^{k} + W_{i+1,j}^{k-1}}{2\Delta\varphi_{+} r_{i+1}^{+}} + \frac{U_{i+1,j}^{k}}{\Delta x_{+}}\left(1 - \frac{r_{i}^{+}}{r_{i+1}^{+}}\right)\right)\right] \tag{13}$$

For $1 \le i \le N-1$, $1 \le k \le L-1$ and $2 \le j \le JMAX-1$

The convergence within the boundary layer is achieved when the following criteria:

$$\left| \frac{\left|X^{(p+1)}\right| - \left|X^{(p)}\right|}{\text{Sup} \ \left|X^{(p+1)}\right|, \left|X^{(p)}\right|} \right| \le \varepsilon \tag{14}$$

is simultaneously checked for T, U and W.

$X^{(p)}$ and $X^{(p+1)}$ are respectively the values of the quantity X of the iterations p and p + 1.

5. Limit The Opening of the Cone

To ensure the validity of the assumption of laminar flow and to further avoid the problem of return of fluid particles, we propose a relationship that brings together the variation ranges of α and θ_o for which, the dimensionless tangential component remains consistently positive. Then, the boundary of the opening of the cone as a function of the inclination α is defined by the following expression:

$$\theta_{0\ \mathrm{limite}} = \pi/2 - (\alpha + 1) \tag{15}$$

We preceded to the verification of the normal component dimensionless V+. It seems negative for $\theta_0 < \alpha$ on the lower meridian equation $\varphi = 0°$, and this indicates the presence of suction. However, to the extent of having a stable and knowing that $\alpha = f(\theta_0)$, we adopted the following condition:

$$\theta_{0\ \mathrm{limite}} \geq \alpha + 1 \tag{16}$$

6. Results and Discussion

In our results, we set Pr=0,72, T_p=373K and $T_\propto$=298K.

We validated the numerical code by comparing the results of our calculations with those deduced from the literature [7]. The figure 2, illustrating the change in temperature at steady state as a function of the normal coordinate y+ at x+=1,0, shows that our results are in good agreement with those in the literature, the relative difference does not exceed 5%.

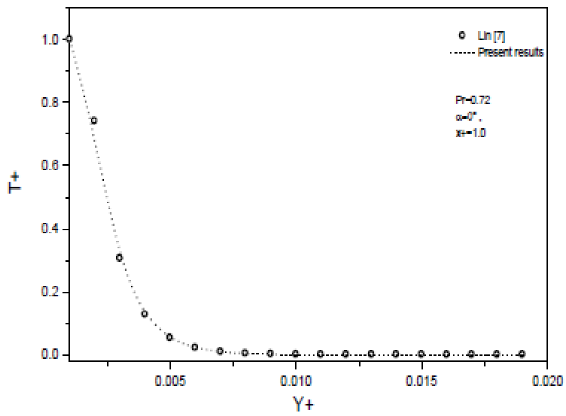

Figure2. *Comparison of steady state temperature profile against y_+ at x+=1,0 and α=0°*

The curves in figure 3.a represent the evolution of the dimensionless meridional component of the velocity as a function of the dimensionless normal coordinate y+ on the upper meridian φ=180°, θ_o=20° and for different values of α. These curves show that the value represented by a peak, is maximum in the vicinity of the apex of the cone and its amplitude decreases as the inclination angle increases. The figure 3.b represents the amplitude also decreases with increasing the opening angle. However, the variations of the opening and inclination angles of the cone affect very little the thickness of the boundary layer. These results are corroborated by the evolution of the dimensionless temperature according to the normal coordinate dimensionless represented by the curves in figure 9.

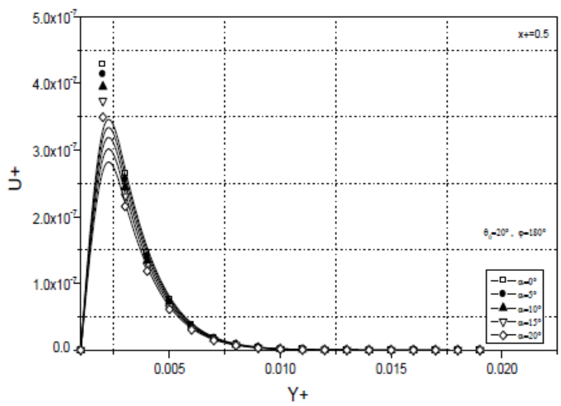

Figure3.a. *Meridian component of the velocity against y_+ at x+=0,5 for different values of α, θ_o=20° and φ = 180°*

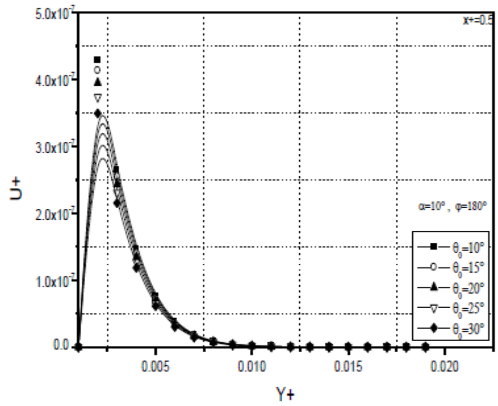

Figure 3.b. *Meridian component of the velocity against y_+ at x_+=0,5 for different values of θ_o, α=10° and φ = 180°*

The figure 4.a shows the evolution of the dimensionless normal component depending on the dimensionless curvilinear coordinate x+ for φ=0°, θ_o=20° and for some values of α. The curves show that it is positive for small values of the inclination (α<20°) and decreases asymptotically toward zero along the wall of the cone. And further, when the inclination angle increases, the normal component becomes negative and its magnitude decreases. It is noted that this component is zero along the lower meridian for values equal to half the opening angle and the angle of inclination of the cone. Moreover, the curves of figure 4.b show that the values of the normal component remains positive on the upper meridian defined by φ=180°, regardless of the inclination and the cone opening. However, this result is found in so far as the inclination angle increases, its grown modulus on this meridian and it decreases when the opening angle increase. The curves of the figure 5.a and figure 5.b corroborate these results. The negative values of the normal component of the velocity characterize the movement of the fluid to the wall on the lower meridian when the cone is strongly inclined (figure 6.a). These results were confirmed by the evolution of this component in function y+ for α=45° and φ=0°, the fluid adheres better on the lower meridian. As against, this bonding tends to disappear with the growth of the opening angle. Then, the fluid is discharged from the wall on the middle and upper meridians, as shown in the curves of the figure 6.b.

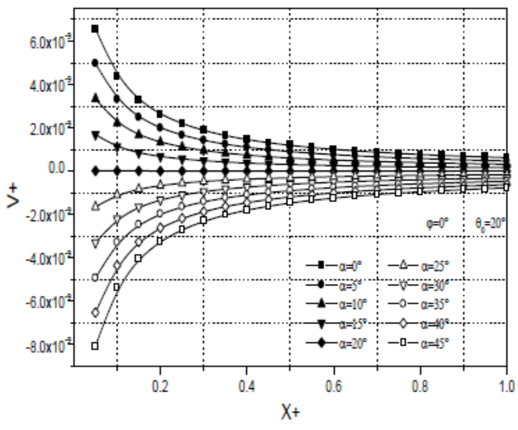

Figure4.a. *Normal component of the velocity against x_+ for different values of α, θ_o = 20° and φ=0°*

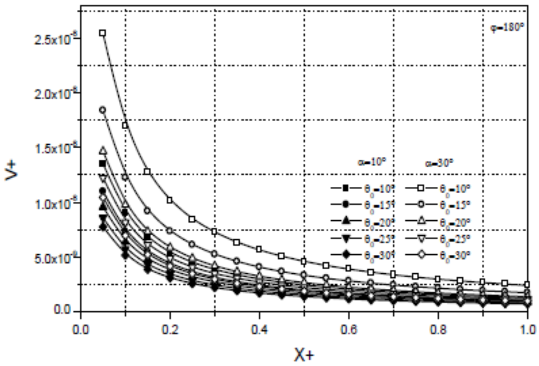

Figure4.b. *Normal component of the velocity against x_+ for different values of θ_o, α = 10° and α=30°, φ=180°*

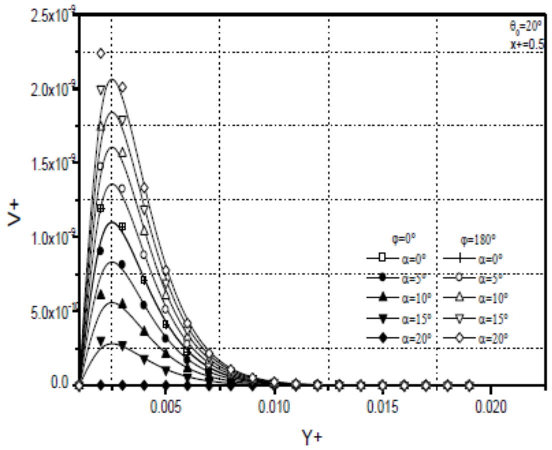

Figure5.a. *Normal component of the velocity against y_+ at x_+=0,5 for different values of α, θ_o=20°, φ=0° and φ=180°*

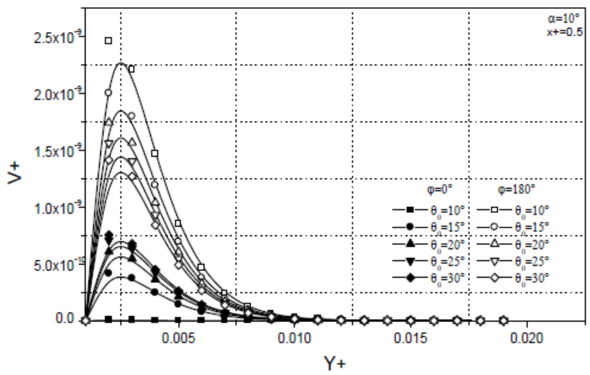

Figure5.b. *Normal component of the velocity against y_+ at x_+=0,5 for different values of θ_o, α=10°, φ=0° and φ=180°*

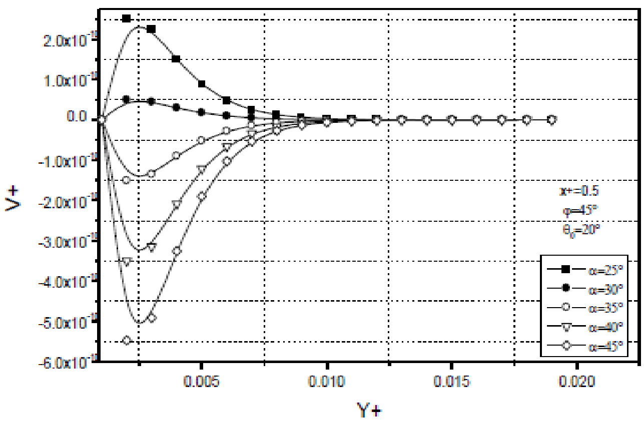

Figure6.a. *Normal component of the velocity against y_+ at x_+=0,5 for different values of α, φ= 45° and θ_o=20°*

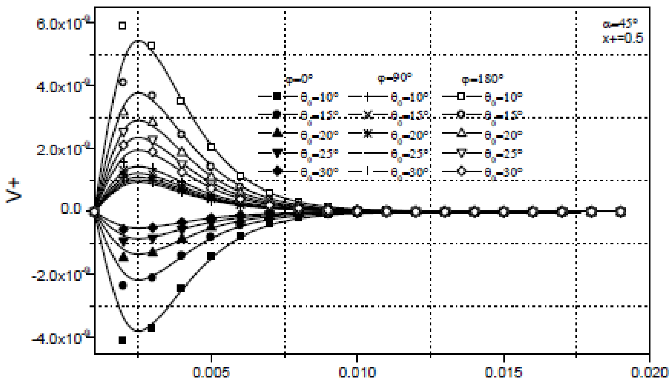

Figure6.b. *Normal component of the velocity against y_+ at x_+=0,5 for different values of θ_o and φ, α=45°*

The figure 7 shows the evolution of the normal component of the velocity depending on the azimuthal coordinate φ for some values of θ_o and the inclination angle. Overall, it varies following a sinusoidal profile and increases from the lower meridian to the upper meridian. Its amplitude increases with the angle of inclination and decreases with the increase of the opening angle θ_o. The curves show that there is a special point in the vicinity of the meridian of equation φ=90° and whose the position depends on the curvilinear abscissa x+, which the normal component does not depend on the angle of inclination or of the opening angle. Moreover, the amplitudes decrease according to the growth of the value of θ_o and x + (Figure 7.b). However, the intensities increase with increasing α and constantly decreases with increase in the value of x + (Figure 7.c). The figure 8, illustrates the variations of the azimuthal component. The module of this component increases with increasing α, however, W + remains unchanged in terms of x +. The presence of substantial aspiration appears when the body is heavily tilted (figure 8.b). The dimensionless azimuthal velocity component varies sinusoidally as a function of φ and the intensities depend and constantly increase with the growth of the inclination angle α. Furthermore, the opening angle at the top has minimal effect on this component (figure 8.d).

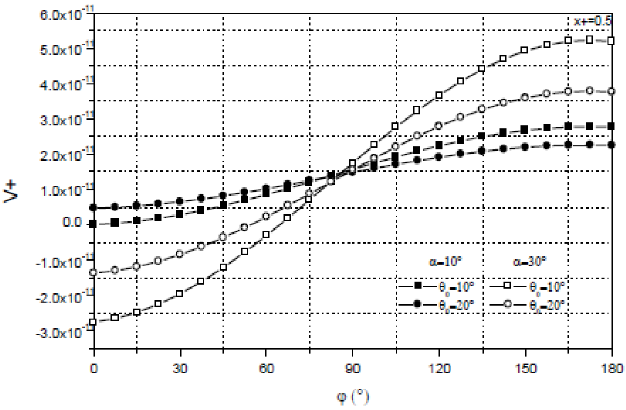

Figure7.a. *Normal component of the velocity against φ at x_+=0,5 for different values of θ_o and α*

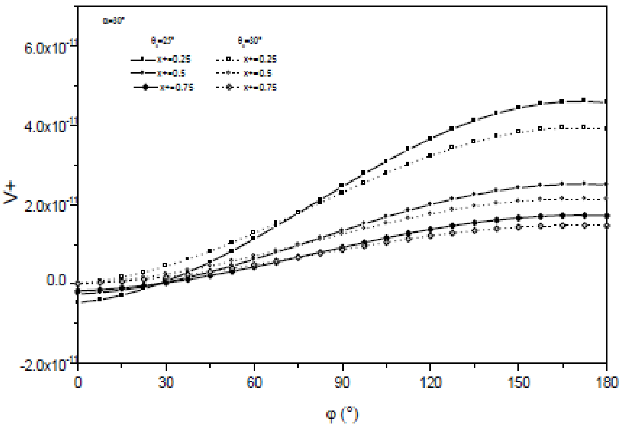

Figure7.b. *Normal component of the velocity against φ, for different values of x+ and θo, α=30°*

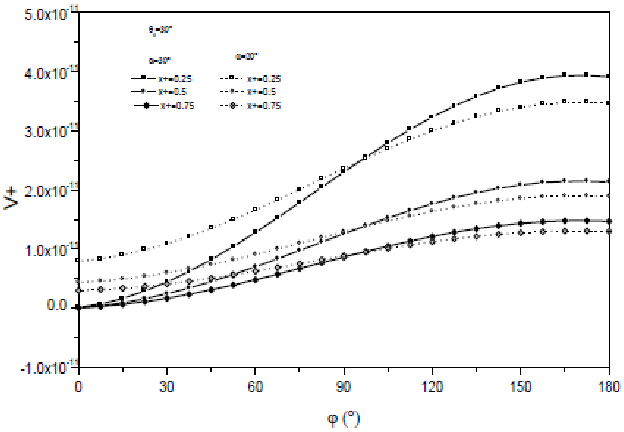

Figure7.c. *Normal component of the velocity against φ, for different values of x_+ and α, θ_o=30°*

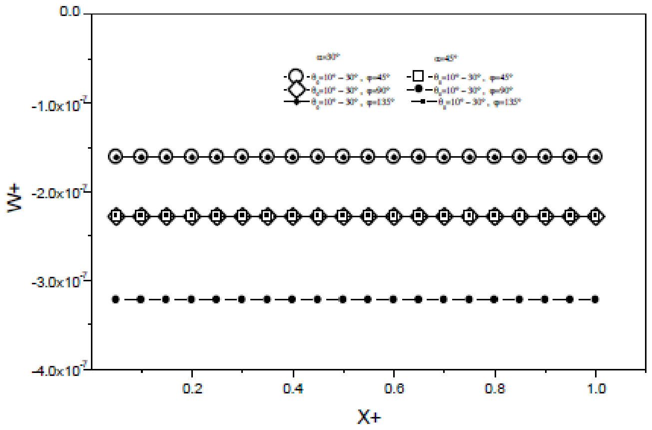

Figure8.a. *azimutal component of the velocity against x+, for different values of* θ_o*,* α *and* φ

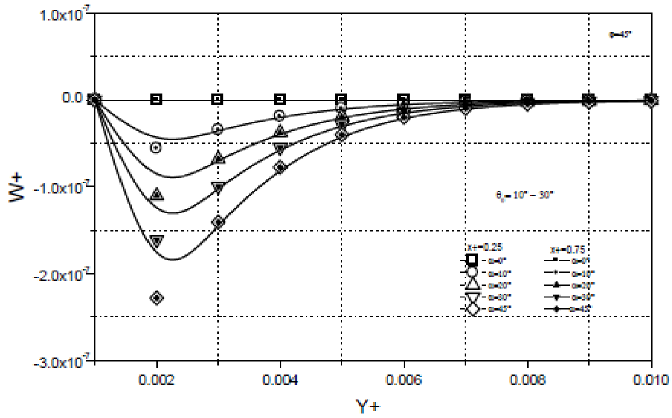

Figure8.b. *azimutal component of the velocity against y+, for different values of* α*,* θ_o *and x+*

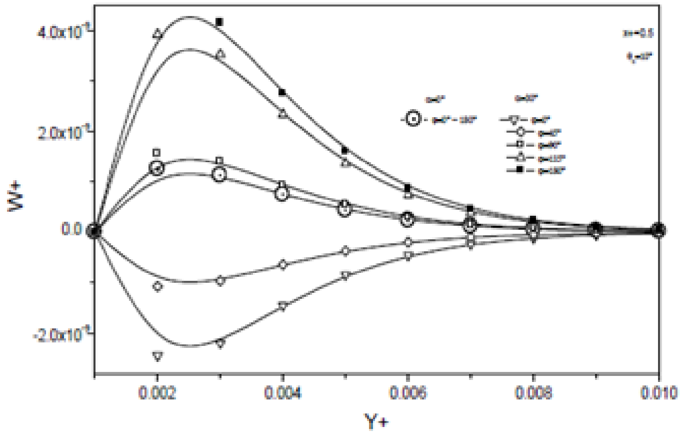

Figure8.c. *azimutal component of the velocity against y+, for different values of* φ *and* α*, for x+=0.5 and* θ_o*=10°*

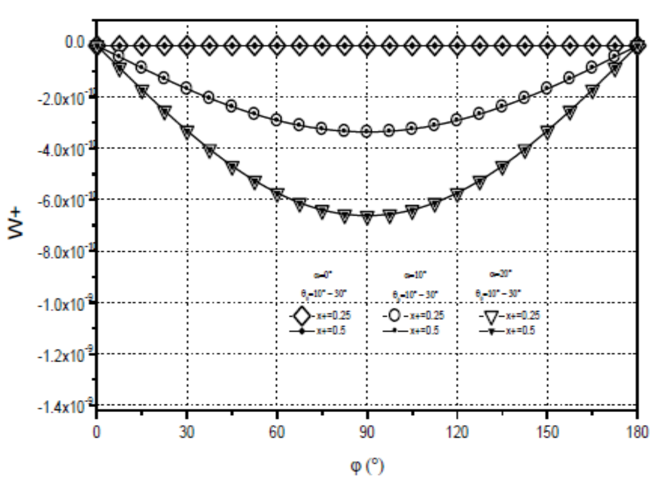

Figure8.d. *azimutal component of the velocity against* φ*, for different values of* θ_o*,* α *and x+*

In this study, the flux is constantly uniform and the heat exchange takes place only according to the normal to the generating surface of the isothermal body. These remarks are confirmed by the curves of figure 10, showing the variations the Nusselt number with y +, for several values of θ_0 and x + on the lower meridian. Therefore, the heat exchange decreases gradually when moving away from the wall and it is independent of θ_0 and x +.

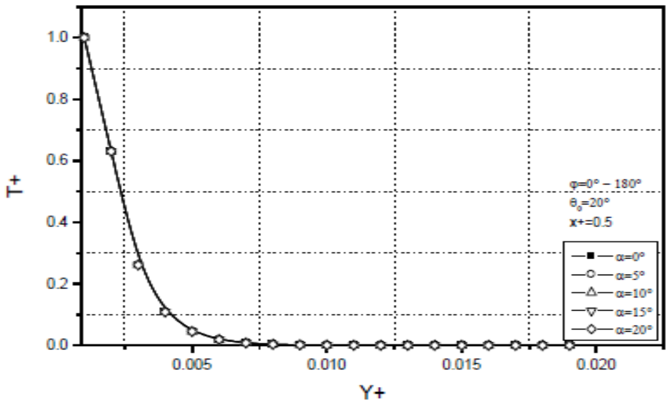

Figure9. *Temperature profile against y_+ at x_+=0,5 for different values of α, φ=0° and φ=180°, for θ_o =20°*

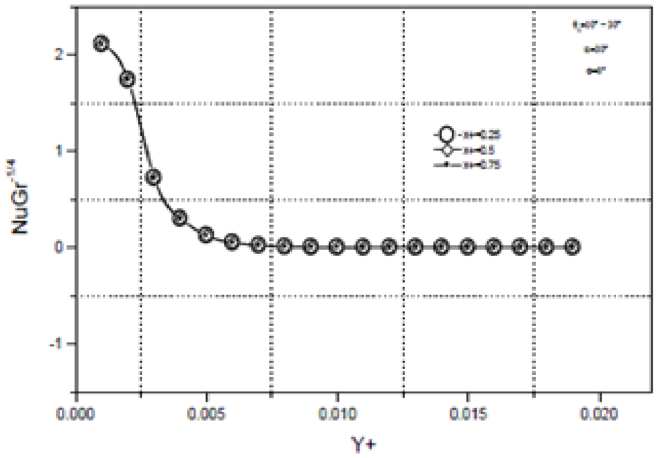

Figure10. *Nusselt number against y+ at φ=0°, for different values of x+ and θ_o, for α=30°*

The curves in figure 11, show that the coefficient of wall friction depending of x+, evolves of sinusoidal manner with φ. Its amplitude grows when the angle of inclination increases and decreases with increase of the opening angle. It seems normal that for the low opening and inclination angles of the cone, the friction tangential coefficient Cfu varies very slightly depending of φ. On the other hand, the azimuthal friction coefficient Cfw also evolves according to a sinusoidal profile with the azimuthal coordinate φ, as shown in figure 12. These curves show that the amplitude increases with the increase of the inclination angle α, while the influence of the opening angle is practically very low, in reason of the symmetrical of revolution of body.

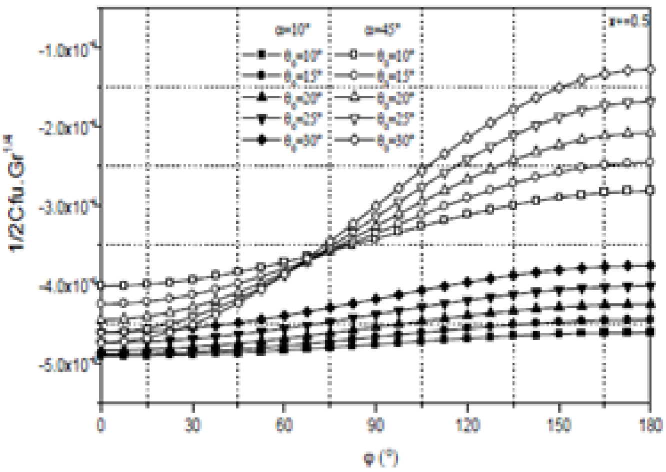

Figure11. *Tangential friction coefficient against φ at x_+=0,5 for different values of θ_o and α*

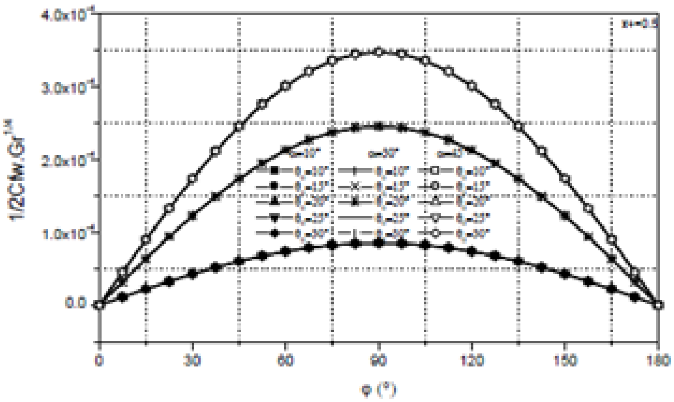

Figure 12. *Azimuthal friction coefficient against φ at x_+=0,5 for different values of θ_o and α*

7. Conclusion

We conducted a numerical study of flow and heat transfer by free convection around a cone of revolution whose axis is inclined relative to the vertical direction and the wall is kept at a constant temperature. We more particularly reported in this article the study of the influence of the opening and the inclination angles of the cone on the normal component of the velocity. Furthermore, our results showed that there is a privileged point situated in the vicinity of the meridian φ = 90° which the normal component is both independent of the inclination and the opening angles of the cone.

However, we noticed that the variation of the opening angle of cone does not affect much on azimuthal friction coefficient, while increasing the inclination angle, its only increases modulus. Moreover, the effects of the inclination and the opening angles of the cone are comparatively very small both on the thickness of the boundary layer that on the heat exchange.

References

[1] Merk H. J., Prins J. A., Thermal convection in laminar boundary layer, Int. Appl. Sci. Res. 4, 11-24 (1953).

[2] Alamgir M., Overall heat transfer from vertical cones in laminar free convection: an approximate method, ASME. J.H.T. 101, 174–176 (1989).

[3] Pullepu B., Ekambavanan K., Chamkha A. J., Unsteady laminar natural convection flow past an isothermal vertical cone, I.J.H.T. 25(2), 17-28 (2007).

[4] Pop, Tsung Yen, Natural convection over a vertical wavy frustum of a cone, I.J.N.M. 34, 925-934 (1999).

[5] Siabdallah M., Zeghmati B., Daguenet M., Etude de la convection naturelle thermique et massique dans la couche limite autour d’un tronc de cône à paroi sinusoïdale, Conference proceeding, 12th J.I.T (2005).

[6] Roy S., Free convection from a vertical cone at high Prandtl numbers. , Trans. A.S.M.E. J.H.T. 96, 115-117 (1974).

[7] Lin F. N., Laminar convection from a vertical cone with uniform surface heat flux, Letters H.M.T. , 49-58 (1976).

[8] Rakotomanga F. A., Alidina E., Transferts thermiques convectifs tridimensionnels autour d’un cône de révolution, Conference proceeding, Congress S.F.T. Ref 6212 (2013).

[9] Alim M. A., Alam M., Chowdhury M. K., Pressure work effect on natural convection flow from a vertical circular cone with suction and non-uniform surface temperature J.M.E. ME 36, 6-11 (2006).

[10] Pop I., Watanabe T., Free convection with uniform suction or injection from a vertical cone for constant wall heat flux, Conference proceeding, Int. Comm. Heat Mass Transfer, Pp 275–283, (1992).

AUTHORS' BIOGRAPHY

Ulrich CANISSIUS, Studies in mechanical engineering and fluid mechanics, energy option. Higher teacher assistant and research. Researcher at the University of Antsiranana, attached to the department of Mechanical and Metrology at the University of Antsiranana, Madagascar.

Edouard ALIDINA, Studies in energy systems and fluid mechanics. Doctor of new regime specialized in solar energy, France. PhD in fluid mechanics, Madagascar. Professor at the Faculty of Science at the University of Antsiranana, Madagascar.